

# Self-training of Machine Learning Models for Liver Histopathology: Generalization under Clinical Shifts

Jin Li, Deepta Rajan, Chintan Shah, Dinkar Juyal, Shreya Chakraborty, Chandan Akiti, Filip Kos, Janani Iyer, Anand Sampat, Ali Behrooz

ALI.BEHROOZ@PATHAI.COM

PathAI, Inc., Boston MA, USA

## Abstract

Histopathology images are gigapixel-sized and include features and information at different resolutions. Collecting annotations in histopathology requires highly specialized pathologists, making it expensive and time-consuming. Self-training can alleviate annotation constraints by learning from both labeled and unlabeled data, reducing the amount of annotations required from pathologists. We study the design of teacher-student self-training systems for Non-alcoholic Steatohepatitis (NASH) using clinical histopathology datasets with limited annotations. We evaluate the models on in-distribution and out-of-distribution test data under clinical data shifts. We demonstrate that through self-training, the best student model statistically outperforms the teacher with a 3% absolute difference on the macro F1 score. The best student model also approaches the performance of a fully supervised model trained with twice as many annotations.

**Keywords:** Histopathology, Self-training, Semi-supervised learning, Generalization, NASH

## 1. Introduction

A pathologist’s diagnosis is often considered as the ground truth for disease detection, staging, and severity scoring. The traditional histopathology workflow involves man-

ual reviewing of a large number of whole-slide images (WSI) to evaluate cell and tissue morphologies. The task is time-consuming and is complicated by high inter and intra-annotator variability (Javed et al., 2022). Machine learning (ML) models have been shown to improve throughput of histopathology workflows in detection and prediction of cancer subtypes, gene mutations (Coudray et al., 2018), and molecular phenotypes (Diao et al., 2021). However, the success of these approaches relies on the quantity and quality of annotations from board-certified pathologists, which are expensive to obtain. The large size of histopathology images also presents a challenge in getting exhaustive annotations. A successful way to navigate this problem is to extract patches from the WSI which has enabled the success of deep learning solutions (Srinidhi et al., 2020). The intrinsic biases in acquiring histopathology images imply that sampling patches from WSIs rarely covers the full data distribution. There exists a number of known confounders causing batch effects (Howard et al., 2021) that stem from variations across tissue sites, patient demographics, hospitals, stains, and scanners. There is also a severe label imbalance due to varying comorbidities within patient populations enrolled in different clinical trials (Thiagarajan et al., 2018).

Semi-supervised learning (SSL) for domain adaptation handles these data-driven constraints by leveraging unlabeled data through pseudo labeling (Lee et al., 2013) to develop accurate and robust models. Several prior works both in natural and medical imaging applications (Zou et al., 2018; Kamnitsas et al., 2021; Rajan et al., 2021) show significant performance gains over fully-supervised methods. However, it is often difficult to exactly define under what conditions SSL works or which modeling components help or hurt performance (Van Engelen and Hoos, 2020). In addition, it is important to investigate how SSL methods can generalize to clinical shifts, as trained histopathology models need to do well on new clinical trials.

## 2. Related Work

Prior work in semi-supervised learning for histopathology image classification has involved model pre-training on large-scale natural image datasets followed by fine-tuning as shown in Marini et al. (2020); Shaw et al. (2020), combining self-supervision with semi-supervision, or exploiting consistency regularization in Srinidhi et al. (2021); Pulido et al. (2020). However, most of these techniques require designing domain-specific pre-training tasks and augmentations.

For AI-based analysis of NASH histopathology, most previous works deploy supervised models with convolutional neural networks (CNN) to segment disease features in WSIs from liver samples. A CNN-based WSI segmentation system was developed by Taylor-Weiner et al. (2021) to measure important histological characteristics of NASH, such as steatosis, inflammation, hepatocellular ballooning, and fibrosis. Heinemann et al. (2019) employed Masson’s Trichrome WSIs to create 4 CNNs that categorize patches into stages of fibrosis, ballooning, inflammation, and steatosis.

The logits from each model were averaged over all the patches of a trichrome WSI to produce the slide level classes. Dwivedi et al. (2022) showed improvements in AI-based NASH scoring by applying fusion models to segmentation masks from NASH Hematoxylin and Eosin (H&E) and Trichrome samples.

To the best of our knowledge, this work is the first effort to analyze the design of semi-supervised learning algorithms for evaluating samples from NASH patients using histopathology WSIs from clinical trials. We show that self-training improves performance over the supervised baseline on both the in-distribution dataset and out-of-distribution clinical trial datasets. We also demonstrate that by using unlabeled data, student models can approach the performance of fully supervised models trained with twice the number of labels.

## 3. Methods

Teacher-student learning paradigms leverage pseudo labels (Lee et al., 2013), and involve the following sequence of steps: (i) train a teacher model on the labeled data, (ii) create pseudo labels on the unlabeled data, (iii) select pseudo labels by filtering them based on some criteria, and (iv) train a student model on both the labeled and pseudo labeled data (see Figure 1). This training paradigm allows the teacher model to distill knowledge from the pre-trained teacher to the student (Hinton et al., 2015). We primarily focus on analyzing the NST and MPL approach and we use the other methods in Section 2 for comparison. See Appendix A for a detailed description of the methods we used. See Appendix B for the modeling framework, including the augmentations we used, calibration methods, model architecture, and pseudo label selection method. And see Ap-

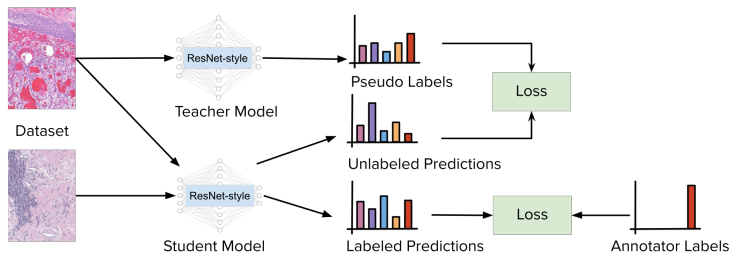


Figure 1: Diagram of how the student model is trained in the teacher-student paradigm. In the training step, the teacher model first creates pseudo labels from the unlabeled data. Then the student model is optimized from the sum of two losses: one based on the unlabeled predictions and the pseudo labels and the other from the labeled predictions and the annotator labels.

pendix C for the hyperparameters we picked to train our teacher student models.

## 4. Experiments

### 4.1. Dataset

**Non-Alcoholic Steatohepatitis:** Non-Alcoholic Steatohepatitis (NASH) is a chronic liver disease linked to obesity and other metabolic diseases, leading to type II diabetes and fibrotic liver [Williams et al. \(2011\)](#). Our dataset consists of digitized liver biopsy slides of varied sizes. These slides are stained by H&E stain and scanned at 40x resolution by Aperio scanners. In this work, we consider the problem of classifying patches extracted from WSIs into one of 13 classes associated with different histologic features in NASH. All slides are partially annotated by board certified pathologists trained in hepatobiliary pathology with one of the 13 classes. These 13 classes are: Bile Duct, Portal Inflammation, Steatosis, Normal Hepatocytes, Hepatocellular Swelling, Lobular Inflammation, Normal, Lumen, Blood Vessels, Interface Hepatitis, Hepatocellular Ballooning, Microvesicular Steatosis, Normal Interface. We sample patches of size 526 x 526 pixels at the highest resolution from these

annotated regions for patch-based learning. The result of the segmentation can then be used in downstream analysis to predict the clinical scores or patient outcomes.

**Dataset Split:** Our empirical study comprises an in-distribution (ID) dataset and three generalization test sets. The WSIs belonging to the ID dataset are obtained from patients belonging to two different randomized control trials, and make up the source domain. We start with 201 patients in our train set, 44 patients in the validation set and 45 patients in our test set. We use patches from the slides of these patients to train the baseline teacher model. To train the student model, we use unlabeled patches from the slides of an additional 202 patients. To see how well our student model performs against a model trained on more labels, we collect labels for those 202 patients and train another model (called the Oracle) on the patches from all 403 patients.

**Evaluation under Clinical Trial Shifts:** The intrinsic variations in data collection cause many challenging distribution shifts to co-exist in histopathology datasets. Potential causes can be shifts in patients population (age, ethnicity, gender, clinical history etc.), prevalence (stage of disease, target se-

Data	Patients	Slides	Patches
Training	403	535	1,136,360
Validation	44	60	60,256
IID Test	45	57	49,842
CT A	44	44	151,814
CT B	14	14	41,688
CT C	94	94	974,529

Table 1: Summary of the histopathology image sample sizes used in our study. Clinical trial (CT) shifts A, B, C are out of distribution data.

lection), data acquisition process (scanner, biopsy thickness, staining protocol) or in annotations (varying expertise of annotators or annotation policy).

Our test set is divided into four subsets: in distribution test consists of images from the same clinical trials that were used in model training and validation. The other three test sets consist of images used in three different clinical trials (CT-A, CT-B, CT-C) that were not used during training. The sizes of the test sets are given in Table 1. Based on NASH scores from human experts, the ID Test is the most severely diseased, while CT-B and CT-C are milder (earlier stage of disease); CT-A is mild in lobular inflammation (LI) and hepatocellular ballooning (HB) but severe in steatosis. There are significant differences in annotation distributions between these sets. While the ID Test has a fairly balanced distribution of classes, the distributions of CT-B and CT-C are very skewed towards non-pathological classes (Normal or Normal Hepatocytes). CT-A on the other hand is rich in annotations of LI and HB, as well as steatosis. Figure 2 gives the distribution shift for the different classes across the various test datasets used.

## 5. Results

We first train the teacher models on patches from the slides of 201 patients and treat that as our baseline. We then used unlabeled patches from an additional 202 patients combined with the patches used in the teacher model to train all of our student models. Finally, we collect annotations for the 202 patients and use all 403 patients to train the oracle. We make the following observations based on our results:

**Student models outperform teacher models on both in distribution and out of distribution data** Based on Table 3, we find that the student models consistently perform better than the teacher model. For example, MPL is 3% better than Teacher on IDD Test set and around 4% better on CT-A, CT-B, and CT-C. This demonstrates that student models can effectively learn from unlabeled data and produce better results than the baseline teacher models.

**Self-training is nearly as good as collecting twice as many expert annotations** We compare one of our best student models, MPL, which only has labels from patches from 201 patients, to the oracle, which has labels from all 403 patients. Despite the fact that the oracle has access to twice as much labeled information as MPL, MPL is able to match the perfor-

Table 2: Notation for models explored in this work. Note that we use (**Teacher**) to develop each of the students.

Model	Description
Teacher	Teacher with augmentation + mixup + dropout
SS+UL ST+FT	Partial labeled + unlabeled loss (conditional entropy + class balance) Pre-train student on pseudo labels and fine-tune on labeled data
NST	Iterative self-training with noisy students
NST+T	NST with temperature scaling
NST+T+U	NST with temperature scaling and UPS method
MPL	Meta pseudo labels
MPL+T	MPL with temperature scaling
Oracle	Trained using 100% labeled data + augmentation + mixup + dropout

mance of the oracle on IDD (macro F1 score of 0.524 vs 0.522). Furthermore, the student model can match the performance on CT-B (0.365 vs 0.367) and CT-C (both have macro F1 scores of 0.474). However, for CT-A, MPL was not able to match performance of the oracle (0.526 vs 0.598). Even the best performing teacher-student training method (NST+T+U) on CT-A (0.549) is unable to match the oracle’s performance on dataset CT-A.

**Evolving second generation students in NST yield greater benefits** In NST, we used the second generation student evolved from the first student, meaning we trained two student models and used the last one for inference. We find that evolving a second student generally adds 1-2% improvement of macro F1 score on the test datasets but any further iterations did not improve performance.

**Calibrated methods do not necessarily improve student models** We tried to further improve our models by improving the calibration of our teacher models with temperature scaling and uncertainty-aware pseudo-label selection (UPS). A better calibrated model will produce better pseudo labels which can then improve which patches are selected during the pseudo label filter-

ing process. The performance of calibrated students NST+T+U and MPL+T is not significantly different than the non-calibrated counterparts NST and MPL (Table 3). We suspect that even though the selected pseudo labeled samples may be better calibrated, they are not any more diverse and thus the student models will not benefit from those unlabeled patches.

## 6. Conclusion

Prohibitively expensive collection of annotations from domain experts and generalizability of trained models under clinical data shifts are two of the major challenges faced in histopathology image analysis and model development. To address this, we train different self-training models that leverages unlabeled data to improve performance on these generalization sets. We evaluate each method on data from three separate clinical trials not used in model training as well as on an in-domain test set. We showed that semi-supervised models can improve significantly over the supervised baseline both on in-domain and out-of-domain test sets. MPL+T model was the most consistent performer out of the methods we explored, beating the teacher on every test set and match-

Table 3: Performance of the teacher model, student models, and oracle across IDD Test and clinical trial shifts CT-A, CT-B, CT-C. Due to imbalance in the datasets, we consider the macro F1 score as the primary metric for deriving performance trends. The bounds reported are 95% confidence intervals obtained by bootstrap analysis. Student models do much better than the teacher and MPL student can match the performance of the oracle on most clinical trial shifts.

Model	IDD Test		CT-A		CT-B		CT-C	
	F1	Bounds	F1	Bounds	F1	Bounds	F1	Bounds
Teacher	0.492	0.487, 0.497	0.481	0.472, 0.491	0.328	0.318, 0.338	0.431	0.428, 0.435
SS+UL	0.482	0.478, 0.486	0.466	0.457, 0.475	0.309	0.300, 0.319	0.408	0.404, 0.411
SS + FT	<b>0.525</b>	0.520, 0.529	0.526	0.516, 0.536	0.327	0.316, 0.338	0.471	0.468, 0.474
NST	0.494	0.490, 0.498	0.540	0.529, 0.551	0.348	0.336, 0.360	0.460	0.456, 0.464
NST+T	0.496	0.492, 0.501	0.512	0.501, 0.523	0.340	0.325, 0.353	0.443	0.440, 0.446
NST+T+U	0.517	0.512, 0.520	<b>0.549</b>	0.538, 0.560	0.329	0.318, 0.341	0.467	0.463, 0.470
MPL	0.524	0.520, 0.529	0.525	0.516, 0.535	<b>0.365</b>	0.353, 0.377	<b>0.474</b>	0.470, 0.477
MPL+T	0.524	0.520, 0.529	0.526	0.516, 0.537	0.363	0.350, 0.376	0.467	0.463, 0.470
Oracle	0.522	0.518, 0.527	0.598	0.588, 0.607	0.367	0.356, 0.379	0.474	0.471, 0.478

ing the performance of Oracle on all but one test set.

In the future, we can explore how to better select unlabeled data to improve the performance of student models on generalization data sets. For example, we can try pre-training a SimCLR model only on unlabeled to get representations of the input images and then use those representations to select a diverse set of unlabeled patches to feed into the student model [Chen et al. \(2020\)](#). We can also try to add in unlabeled data from different clinical trials to see how much that improves generalization performance on out of distribution clinical trial shifts.

Overall, self-training has shown a potential to significantly reduce the amount of labeled data required in histopathology image

analysis without compromising model performance and generalizability.

## Acknowledgments

Thanks to Aryan Pedawi, Diksha, Tanmaya, John, Chaitanya, Zahil, and Aaditya Prakash for their comments and support. Also, special thanks to Ben Trotter for the excellent assistance on datasets, and to Murray Resnick and Fedaa Najdawi for their expert inputs on histopathology.

## References

Ting Chen, Simon Kornblith, Mohammad Norouzi, and Geoffrey E. Hinton. A simple framework for contrastive learn-

- ing of visual representations. *ArXiv*, abs/2002.05709, 2020.
- Nicolas Coudray, Paolo Santiago Ocampo, Theodore Sakellaropoulos, Navneet Narula, Matija Snuderl, David Fenyő, Andre L Moreira, Narges Razavian, and Aristotelis Tsirigos. Classification and mutation prediction from non-small cell lung cancer histopathology images using deep learning. *Nature medicine*, 24(10):1559–1567, 2018.
- James A Diao, Jason K Wang, Wan Fung Chui, Victoria Mountain, Sai Chowdary Gullapally, Ramprakash Srinivasan, Richard N Mitchell, Benjamin Glass, Sara Hoffman, Sudha K Rao, et al. Human-interpretable image features derived from densely mapped cancer pathology slides predict diverse molecular phenotypes. *Nature communications*, 12(1):1–15, 2021.
- Chaitanya Dwivedi, Shima Nofallah, Maryam Pouryahya, Janani Iyer, Kenneth Leidal, Chuhan Chung, Timothy Watkins, Andrew Billin, Robert Myers, John Abel, and Ali Behrooz. Multi stain graph fusion for multimodal integration in pathology. In *Proceedings of the IEEE/CVF Conference on Computer Vision and Pattern Recognition (CVPR) Workshops*, pages 1835–1845, June 2022.
- Geoffrey French, Michal Mackiewicz, and Mark Fisher. Self-ensembling for visual domain adaptation. *arXiv preprint arXiv:1706.05208*, 2017.
- Y. Gal and Zoubin Ghahramani. Dropout as a bayesian approximation: Representing model uncertainty in deep learning. *ArXiv*, abs/1506.02142, 2016.
- Fabian Heinemann, Gerald Birk, and Birgit Stierstorfer. Deep learning enables pathologist-like scoring of NASH models. *Scientific Reports*, 9(1), December 2019. doi: 10.1038/s41598-019-54904-6. URL <https://doi.org/10.1038/s41598-019-54904-6>.
- Geoffrey E. Hinton, Oriol Vinyals, and J. Dean. Distilling the knowledge in a neural network. *ArXiv*, abs/1503.02531, 2015.
- Frederick M Howard, James Dolezal, Sara Kochanny, Jefree Schulte, Heather Chen, Lara Heij, Dezheng Huo, Rita Nanda, Olu-funmilayo I Olopade, Jakob N Kather, et al. The impact of site-specific digital histology signatures on deep learning model accuracy and bias. *Nature communications*, 12(1):1–13, 2021.
- Syed Ashar Javed, Dinkar Juyal, Zahil Shannis, Shreya Chakraborty, Harsha Pokkalla, and Aaditya Prakash. Rethinking machine learning model evaluation in pathology. *arXiv preprint arXiv:2204.05205*, 2022.
- Konstantinos Kamnitsas, Stefan Winzeck, Evgenios N Kornaropoulos, Daniel Whitehouse, Cameron Englman, Poe Phyu, Norman Pao, David K Menon, Daniel Rueckert, Tilak Das, et al. Transductive image segmentation: Self-training and effect of uncertainty estimation. In *Domain Adaptation and Representation Transfer, and Affordable Healthcare and AI for Resource Diverse Global Health*, pages 79–89. Springer, 2021.
- Dong-Hyun Lee et al. Pseudo-label: The simple and efficient semi-supervised learning method for deep neural networks. In *Workshop on challenges in representation learning, ICML*, volume 3, page 896, 2013.
- Nicolò Marini, Sebastian Otálora, Henning Müller, and Manfredo Atzori. Semi-supervised learning with a teacher-student paradigm for histopathology classification: A resource to face data heterogeneity and lack of local annotations. In *ICPR Workshops (1)*, pages 105–119, 2020.

- Avital Oliver, Augustus Odena, Colin A Raffel, Ekin Dogus Cubuk, and Ian Goodfellow. Realistic evaluation of deep semi-supervised learning algorithms. *Advances in neural information processing systems*, 31, 2018.
- Hieu H. Pham, Qizhe Xie, Zihang Dai, and Quoc V. Le. Meta pseudo labels. *ArXiv*, abs/2003.10580, 2020.
- J Vince Pulido, Shan Guleria, Lubaina Ehsan, Matthew Fasullo, Robert Lippman, Pritesh Mutha, Tilak Shah, Sana Syed, and Donald E Brown. Semi-supervised classification of noisy, gigapixel histology images. In *2020 IEEE 20th International Conference on Bioinformatics and Bioengineering (BIBE)*, pages 563–568. IEEE, 2020.
- Deepta Rajan, Jayaraman J Thiagarajan, Alexandros Karargyris, and Satyananda Kashyap. Self-training with improved regularization for sample-efficient chest x-ray classification. In *Medical Imaging 2021: Computer-Aided Diagnosis*, volume 11597, page 115971S. International Society for Optics and Photonics, 2021.
- M. N. Rizve, Kevin Duarte, Y. Rawat, and M. Shah. In defense of pseudo-labeling: An uncertainty-aware pseudo-label selection framework for semi-supervised learning. *ArXiv*, abs/2101.06329, 2021.
- Shayne Shaw, Maciej Pajak, Aneta Lisowska, Sotirios A Tsaftaris, and Alison Q O’Neil. Teacher-student chain for efficient semi-supervised histology image classification. *arXiv preprint arXiv:2003.08797*, 2020.
- Chetan L Srinidhi, Ozan Ciga, and Anne L Martel. Deep neural network models for computational histopathology: A survey. *Medical Image Analysis*, page 101813, 2020.
- Chetan L Srinidhi, Seung Wook Kim, Fu-Der Chen, and Anne L Martel. Self-supervised driven consistency training for annotation efficient histopathology image analysis. *arXiv preprint arXiv:2102.03897*, 2021.
- Amaro Taylor-Weiner, Harsha Pokkalla, Ling Han, Catherine Jia, Ryan Huss, Chuhan Chung, Hunter Elliott, Benjamin Glass, Kishalve Pethia, Oscar Carrasco-Zevallos, et al. A machine learning approach enables quantitative measurement of liver histology and disease monitoring in nash. *Hepatology*, 2021.
- Jayaraman J Thiagarajan, Deepta Rajan, and Prasanna Sattigeri. Understanding behavior of clinical models under domain shifts. *arXiv preprint arXiv:1809.07806*, 2018.
- Sunil Thulasidasan, Gopinath Chennupati, Jeff A Bilmes, Tanmoy Bhattacharya, and Sarah Michalak. On mixup training: Improved calibration and predictive uncertainty for deep neural networks. *Advances in Neural Information Processing Systems*, 32, 2019.
- Jesper E Van Engelen and Holger H Hoos. A survey on semi-supervised learning. *Machine Learning*, 109(2):373–440, 2020.
- Christopher D Williams, Joel Stengel, Michael I Asike, Dawn M Torres, Janet Shaw, Maricela Contreras, Cristy L Landt, and Stephen A Harrison. Prevalence of nonalcoholic fatty liver disease and non-alcoholic steatohepatitis among a largely middle-aged population utilizing ultrasound and liver biopsy: a prospective study. *Gastroenterology*, 140(1):124–131, 2011.
- Qizhe Xie, E. Hovy, Minh-Thang Luong, and Quoc V. Le. Self-training with noisy



student improves imagenet classification. *2020 IEEE/CVF Conference on Computer Vision and Pattern Recognition (CVPR)*, pages 10684–10695, 2020.

Hongyi Zhang, Moustapha Cissé, Yann Dauphin, and David Lopez-Paz. mixup: Beyond empirical risk minimization. *ArXiv*, abs/1710.09412, 2018.

Yang Zou, Zhiding Yu, BVK Kumar, and Jinsong Wang. Unsupervised domain adaptation for semantic segmentation via class-balanced self-training. In *Proceedings of the European conference on computer vision (ECCV)*, pages 289–305, 2018.

## Appendix A. Teacher Student Methods

Here we describe in detail the methods of teacher student training. Let  $T$  and  $S$  represent the teacher and student models with model weights  $\theta_T$  and  $\theta_S$  respectively. Let  $D_L = \{(x_l, y_l)\}_{i=1}^{N_L}$  be the labeled set with  $N_L$  number of labeled samples, where  $x_i$  denotes an input image patch and  $y_i \in \mathbb{R}^C$  corresponds to the one-hot label with  $C$  classes. Similarly, let  $D_U = \{(x_u)\}_{i=1}^{N_U}$  be the unlabeled set with a total of  $N_U$  samples. Further, we denote  $\hat{y} = T(x_u; \theta_T)$  as the soft predictions of the teacher model on unlabeled data (i.e. the pseudo-label) and define  $S(x_l; \theta_S)$  and  $S(x_u; \theta_S)$  as student predictions for the labeled and unlabeled data. Let  $D_P = \{(x_u, \hat{y})\}_{i=1}^{N_U}$  be the pseudo labeled dataset. Lastly the cross-entropy between two distributions  $a, b$  is represented by  $CE(a, b)$ .

Formally, we first optimize the teacher weights as in equation 1, construct the pseudo labeled set  $D_P$ , and then filter pseudo labels to form a subset  $D_{P^*}$ . Finally, we train the student model on both the labeled and

pseudo labeled set  $D_B = D_L \cup D_{P^*}$  as in equation 2.

$$\theta_T = \operatorname{argmin}_{\theta} \mathbb{E}_{x_l, y_l} [CE(T(x_l; \theta); y_l)] \quad (1)$$

$$\theta_S = \operatorname{argmin}_{\theta} \mathbb{E}_{x_i, y_i \in D_B} [CE(S(x_i; \theta); y_i)] \quad (2)$$

### A.1. Noisy Student Training (NST)

NST proposed by Xie et al. (2020) builds on the basic premise of teacher-student training by adding additional noise to the teacher or student models. The student models are also evolved over generations by turning the student into the teacher for subsequent iterations. We use both data and model noise, which includes data augmentation, dropout and mixup. We only perform two iterations of this training as students from subsequent generations did not noticeably improve performance similar to the finding in Rajan et al. (2021).

### A.2. Meta Pseudo Labels (MPL)

The teacher’s weights are not updated during student training in NST. Pham et al. (2020) in their work trained the student and teacher simultaneously to allow the teacher to improve based on how well the student performs. In general, the optimal student parameters  $\theta_S$  always depend on the teacher parameters  $\theta_T$ , since the student learns from the pseudo labels of the teacher. We refer to the original paper for more details on the algorithm.

### A.3. Semi-supervised Learning with Labeled + Unlabeled Loss (SS + UL)

French et al. (2017) train their models with a cross-entropy loss for labeled samples and

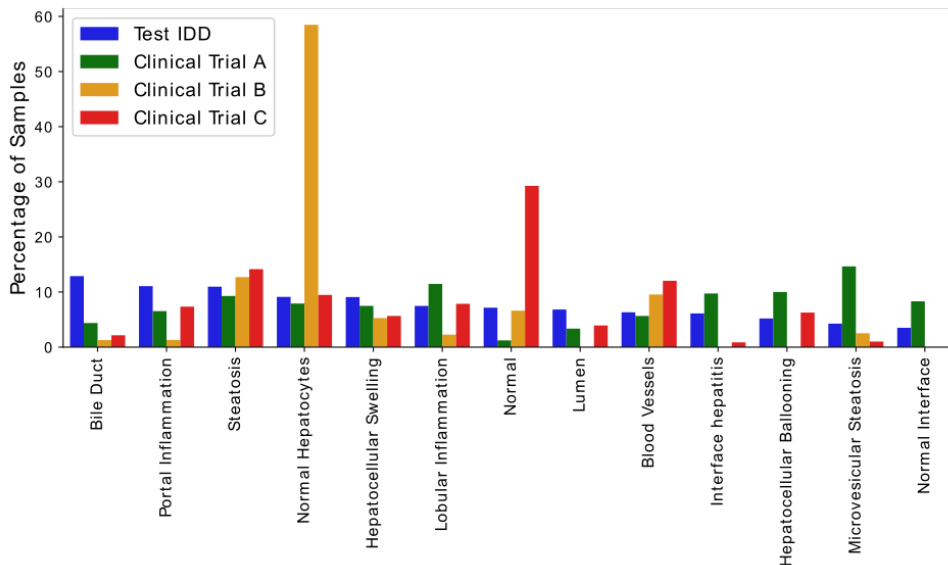


Figure 2: Percentage of samples belonging to each of the 13 classes in the test sets.

an additional loss for the unlabeled samples. In particular, a conditional entropy loss is used to force high-confidence predictions for unlabeled samples, and a class balance loss is used to deal with class imbalance. During our experiment, both unlabeled loss terms are given a weight of 0.2.

#### A.4. Semi-supervised Learning with Fine-tuning (SS + FT)

We also compare the previous methods to another SSL approach proposed by [Marini et al. \(2020\)](#) in the context of histopathology. The teacher is trained from scratch on the labeled data and used to produce pseudo labels for the unlabeled data. However, in this case, the student is pre-trained on the filtered pseudo-labels and further fine-tuned on the labeled set.

## Appendix B. Modeling Framework

We provide descriptions of various factors that impact performance of these self-training algorithms in the following sections

and demonstrate how well self-training methods can generalize to unseen distributions.

**Augmentations:** During training, we augment both labeled and unlabeled patches for all models using flip, rotation, color distortions (brightness, contrast, saturation, hue) and noise corruptions. No augmentations were performed during test.

**Calibration:** We use two calibration techniques to ensure the trained models are more reliable under data shifts. (i) Mixup ([Zhang et al., 2018](#)) is a popular approach that linearly interpolates between a pair of samples and their corresponding labels. Mixup enables regularization of neural network and improves model calibration as shown in [Thulasidasan et al. \(2019\)](#). (ii) Temperature Scaling ([Hinton et al., 2015](#)) scales the logits output from a network by a single parameter to adjust the entropy of a prediction.

**Model Architecture:** The backbone architecture for all models used in our study is a custom 21-layer, ResNet-style convolutional neural network with residual connections. Each block consists of a convolution

layer, a batch norm layer, and a ReLU activation unit. The model has about 13.2 million parameters. Motivated by [Oliver et al. \(2018\)](#), we use the same network for both the teacher and the student to evaluate benefits of self-training without introducing confounding factors like model capacity. We detailed more of the model hyperparameter choices in [Appendix C](#).

**Pseudo-label Selection:** A crucial step in teacher-student self-training is choosing the criteria for filtering pseudo labels to reduce the noise from the unlabeled data. We consider two different approaches to select pseudo labels. (i) Confidence thresholding : We remove pseudo labels if their confidence (probability of the most likely class) is less than some threshold  $k$ ; (ii) Uncertainty-aware Pseudo-label Selection (UPS) : We remove pseudo labels where their MC dropout uncertainty is above a threshold ([Rizve et al., 2021](#)). To compute the uncertainty for a single sample, we perform multiple forward passes with dropout enabled to produce a set of predictions and then compute the standard deviation of those predictions ([Gal and Ghahramani, 2016](#)).

## Appendix C. Training hyperparameters

We tune the teacher model for optimal hyperparameters based on the best macro F1 on the validation set and then use the same hyperparameters for the student models. Any additional hyperparameters specific to the student model, such as temperature and confidence threshold, are tuned on the same validation set. For the teacher model, we conducted ablation studies using augmentations, calibration techniques and dropout. The teacher model that contained augmentations, mixup and dropout performed best, and this model was subsequently used for training students.

All models are trained using the Adam optimizer with a learning rate of 0.0001, a cross entropy loss objective, and a dropout of 0.5. The momentum for batch norm is set to 0.6. We also set the maximum number of iterations to 30,000 and decay the learning rate by 0.5 every 10,000 steps. We use a batch size of 128 for teacher models, and student models use a batch size of 64 for both labeled and unlabeled data. When using mixup, the amount of interpolation controlled by the  $\alpha$  parameter is set to 0.2 ([Zhang et al., 2018](#)). For NST, we used a confidence threshold of 0.4, a temperature of 1.05, and evolved at most 2 generations of student models. For MPL, we used a confidence threshold of 0.2 and a temperature of 1.10. For all teacher-student training methods, we use soft pseudo labels instead of hard pseudo labels since soft pseudo labels performed better in our experiments. When using the UPS method, the uncertainty threshold is set to 0.10 and we performed 10 forward passes for computing the standard deviation.